CHALMERS

UNIVERSITY OF TECHNOLOGY

Laser Frequency Combs for Coherent Optical Communications

(article starts on next page)

Laser Frequency Combs for Coherent Optical Communications

Victor Torres-Company, *Senior Member, OSA*, Jochen Schröder, *Senior Member, OSA, Member, IEEE*, Attila Fülöp, Mikael Mazur, *Student Member, OSA, Student Member, IEEE*, Lars Lundberg, *Student Member, OSA*, Óskar B. Helgason, *Student Member, OSA*, Magnus Karlsson, *Fellow, OSA, Senior Member, IEEE*, and Peter A. Andrekson, *Fellow, OSA, Fellow, IEEE*

Abstract— **Laser frequency combs with repetition rates on the order of 10 GHz and higher can be used as multi-carrier sources in wavelength-division multiplexing (WDM). They allow replacing tens of tunable continuous-wave lasers by a single laser source. In addition, the comb's line spacing stability and broadband phase coherence enable signal processing beyond what is possible with an array of independent lasers. Modern WDM systems operate with advanced modulation formats and coherent receivers. This introduces stringent requirements in terms of signal-to-noise ratio, power per line and optical linewidth which can be challenging to attain for frequency comb sources. Here, we set quantitative benchmarks for these characteristics and discuss tradeoffs in terms of transmission reach and achievable data rates. We also highlight recent achievements for comb-based superchannels, including >10 Tb/s transmission with extremely high spectral efficiency, and the possibility to significantly simplify the coherent receiver by realizing joint digital signal processing. We finally discuss advances with microresonator frequency combs and compare their performance in terms of flatness and conversion efficiency against state-of-the-art electro-optic frequency comb generators. This contribution provides guidelines for developing frequency comb sources in coherent fiber-optic communication systems.**

Index Terms — **Laser frequency combs, coherent communications, wavelength division multiplexing, fiber-optic communication systems, microresonator frequency combs.**

I. INTRODUCTION

A frequency comb is a laser source whose optical spectrum is made of evenly spaced, narrow and phase-locked frequency lines. The comb has two degrees of freedom (stretching and shifting), controlled respectively by two frequencies: the line spacing (or repetition rate), which sets the difference between consecutive lines, and the offset frequency, which defines the location of the comb lines with respect to an ideal grid of frequencies. Key developments in the 90s allowed establishing a coherent link between the frequency comb lines and atomic frequency references [1,2]. This remarkable achievement enabled comparisons between optical clocks with unprecedented precision and accuracy [3], and created opportunities in multiple fields, e.g. broadband molecular spectroscopy [4], the synthesis of pure microwaves [5] and light

detection and ranging [6].

Laser frequency combs have also been widely used in lightwave communication systems, particularly in wavelength division multiplexing (WDM). Results range from on-off keying [7,8] to modern communication systems using advanced modulation formats in single- [9,10] and multi-core fibers [11]. The enabling aspect of frequency combs in WDM systems is the possibility to attain multiple frequency carriers on a fixed grid. Locking the absolute location of the frequency lines to an atomic reference is less relevant. However, the possibility to attain broadband phase coherence and high relative-frequency stability yields advantages compared to what is possible with individual lasers. These advances include mitigation of the inter-channel linear crosstalk [12], compensation of nonlinear impairments in the fiber link by proper waveform shaping [13] or digital pre-distortion [14,15], and the achievement of densely packed superchannels for multi-terabit-per-second transmitters [16,17].

The specifics of modern communication systems introduce tough requirements on the frequency comb in terms of repetition rate, optical linewidth, power per line, spectral smoothness (power distribution among lines) and compatibility with fiber-optic components. These demands offer opportunities for alternative frequency comb platforms [18], such as those based on electro-optic modulation of continuous-wave lasers [8,17,19], gain-switched laser diodes [20], semiconductor-waveguide passively mode-locked lasers [21], fiber-based actively mode-locked lasers [16,22] and microresonator frequency combs [23,24].

The aim in this paper is to set quantitative benchmarks for combs in WDM coherent communication systems. We consider the comb as a black box i.e., for the sake of generality, we focus on requirements that are platform-independent. The analysis carried out in Sect. II reviews the fundamental tradeoffs and limitations with regards to optical signal-to-noise ratio (OSNR), linewidth, relative frequency uncertainty and absolute frequency accuracy. This work therefore complements our

The authors are with the Department of Microtechnology and Nanoscience and the Fiber-Optic Research Center (FORCE), Chalmers University of Technology, SE 41296 Gothenburg, Sweden. Contact e-mail: torresv@chalmers.se.
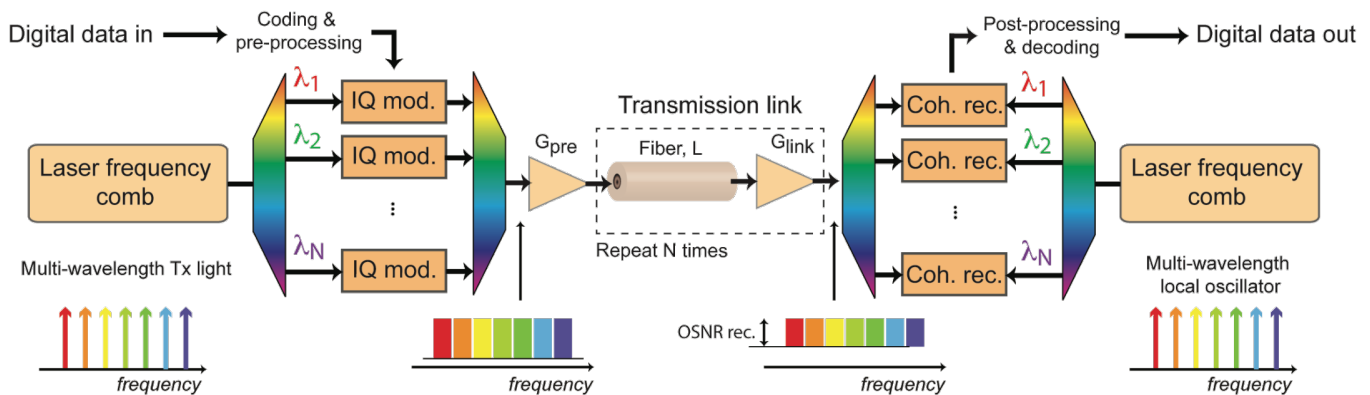
Fig. 1. Schematic of a wavelength division multiplexed coherent communication system where the optical carriers are provided by a frequency comb source.

recent review [25] and extends the conference contribution [26]. In Sect. III, we briefly discuss recent examples at the system level enabled by the unique properties of frequency combs. Finally, in Sect. IV, we establish a comparative assessment of the performance of two relevant comb platforms, namely electro-optic comb generators and microresonator frequency combs, in terms of power conversion efficiency and spectral flatness.

II. PERFORMANCE REQUIREMENTS OF FREQUENCY COMBS IN WAVELENGTH DIVISION MULTIPLEXING

We consider a comb-based WDM point-to-point link as sketched in Fig. 1. The lines of a frequency comb constitute the optical carriers on which to encode data. The demultiplexing stage separates the comb lines, allowing them to be treated as individual continuous-wave sources by the following modulators. The digital data is encoded onto complex symbols which modulate the amplitude and phase of each optical carrier in an IQ modulator. A single polarization is depicted for simplicity, but polarization multiplexing could be implemented e.g. by replicating the transmitter and rotating its polarization after the last multiplexing stage [27]. After multiplexing, the signal is amplified in an erbium-doped fiber amplifier (EDFA) with suitable gain, G_{pre}, to reach the desired power prior to transmission over a fiber link. The link consists of N spans and the losses in every span are compensated for by another EDFA with gain G_{link}. The accumulated spontaneous emission from the EDFAs will degrade the received optical signal to noise ratio, $OSNR_{rec}$. At the receiver side, each channel is demultiplexed and the waveforms are detected in a coherent receiver with the aid of a narrow-linewidth local oscillator whose frequency is matched to the channel of interest. Note that owing to the symmetry at the receiver side, another frequency comb could be used as multi-wavelength local oscillator. The WDM channels in the system of Fig. 1 are detected individually. From this point of view, there is no difference between operating the system with two frequency comb sources or two arrays of tunable continuous-wave lasers, and the fundamentals of coherent optical communications [28] apply equally. In the next section we will consider the possibility of realizing joint signal processing between WDM channels. This can e.g. relax the linewidth requirements [25]. Hence, the

performance metrics analyzed in this section should be taken as an upper limit.

Advanced modulation formats allow encoding more bits per complex symbol. This comes at the expense of a higher requirement in signal to noise ratio (SNR) [29]. An amplified coherent link can, as a first approximation, be modeled as an additive white Gaussian channel, where the noise stems from the optical amplifiers. Fig. 2(a) illustrates the achievable bit error ratio (BER) for different modulation formats as the SNR varies. Adding two bits per symbol requires roughly 6 dB extra SNR to maintain the same BER. These SNR requirements represent a theoretical minimum because the calculation assumes an ideal transmitter and receiver, and ignores nonlinearities in the fiber link. In practice, the digital-to-analog converters in the transmitter and the analog-to-digital converters at the receiver will have a limited number of effective bits. Such imperfections are more acute for advanced modulation formats and higher symbol rates. As a result, higher SNRs than what is set in Fig. 2(a) are needed to attain the same BER [29]. The difference between the theoretical minimum and the actual SNR is called implementation penalty.

Modern high-spectral-efficiency transmission systems apply forward-error-correction (FEC) coding to reach error-free transmission, which is defined as a BER $\leq 10^{-15}$. They typically operate at relatively modest SNRs corresponding to pre-FEC (before decoding) BERs on the order of a few percent and use an overhead of $20 - 30$ percent redundant information to attain error-free post-FEC (after decoding) BERs. However, the relationship between pre- and post-FEC BERs, as well as the required overhead and complexity is highly specific for the selected code. Moreover, the increasingly common *soft decision* codes decode bits based on the received bit probabilities ('soft' data) rather than the 'hard' bit values. Thus, the pre-FEC BER does neither exist nor make sense to use in such cases. This problem has motivated the use of alternative metrics to the pre-FEC BER. One metric that is becoming increasingly popular in the long-haul optical transmission community is the *generalized mutual information* (GMI) [30,31], which will be used in this paper. The GMI is computed from the transmitted and received bit probability distributions. Under some simplifying assumptions the GMI is the maximum data rate (in bits/symbols) the channel can sustain at a given
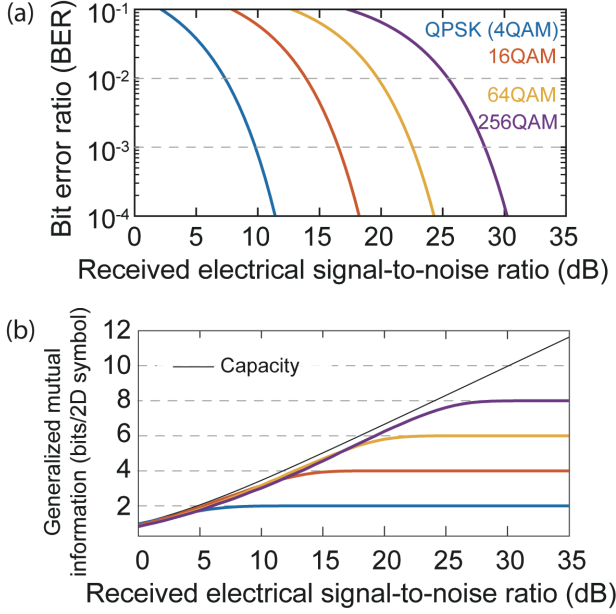
Fig. 2. (a) Achievable bit error ratio as function of signal to noise ratio for different *M*-ary quadrature amplitude modulation (QAM) [32]. (b) Generalized mutual information for the same modulation formats, compared to Shannon's capacity. In both cases, the noise is considered additive and white, following a Gaussian distribution. The GMI is computed assuming bitwise receiver processing, independent bits, and ideal FEC encoding/decoding that can give arbitrary low BER.

SNR and modulation format [see Fig. 2(b)].

A. Optical signal to noise ratio (OSNR)

One practical problem of using a frequency comb instead of an array of tunable lasers is that the comb power is divided among multiple carriers. The lower power in the comb lines directly leads to a decreased SNR. In addition, the comb may display power variations from line to line. To compensate for this, we assume that, following the last multiplexing stage in the transmitter and preamplifier (see Fig. 1), the WDM channels would be equalized (for example with a programmable filter) to achieve an equal target launch power. In this sub-section, we analyze the OSNR performance for the weakest channel in the WDM system which therefore provides a lower bound for the overall system performance.

To calculate the received OSNR, $OSNR_{rec}$, we need to calculate both the received signal power, P_{launch}, and the received noise power, P_{noise}, [33]

$$P_{launch} = P_{low}G_{pre} \qquad (1)$$

Here, P_{low} represents the power level of the weakest WDM channel and G_{pre} the pre-amplifier gain. On the other hand,

$$P_{noise} = n_{sp}h\nu\Delta\nu(G_{pre} - 1 + NG_{link} - N) , \qquad (2)$$

where n_{sp} is the spontaneous emission factor, h the Planck's constant, ν the optical frequency of the channel, $\Delta\nu$ the noise bandwidth and N the number of spans. The received OSNR then becomes
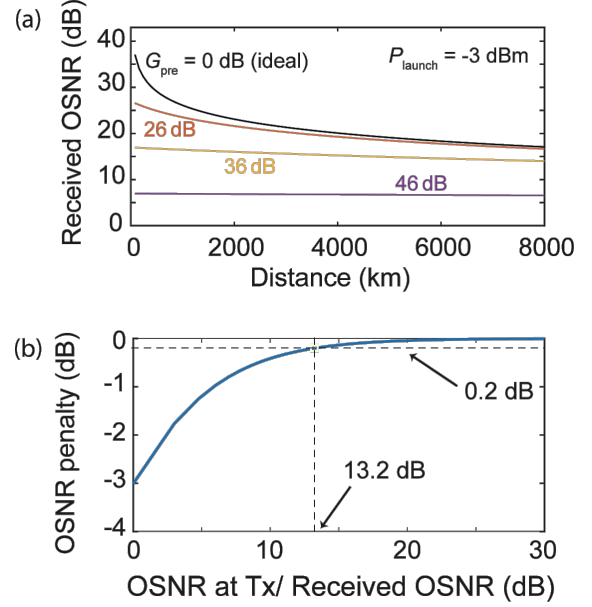
Fig. 3. (a) Evolution of optical signal to noise ratio of a WDM channel with distance for different pre-amplifier gains. The link is formed by consecutive spans of 80 km fiber with 0.2dB/km loss. The noise bandwidth is considered 12.5 GHz and the noise figure of the amplifiers 5 dB ($n_{sp} =$ 1.58). (b) Ratio between OSNR achieved in a power-limited WDM transmitter ($OSNR_{rec}$) and OSNR achieved when pre-amplifier is not needed ($OSNR_{laser}$). This is plotted for different ratio of OSNR at the transmitter side. This result gives the useful rule of thumb that the OSNR at the transmitter side should be 13 dB or higher than the target OSNR at the receiver to be able to ignore potential penalties due to having limited power at the transmitter.

$$OSNR_{rec} = \frac{P_{launch}}{n_{sp}h\nu\Delta\nu(G_{pre} - 1 + NG_{link} - N)} . \qquad (3)$$

Figure 3(a) illustrates how the received OSNR degrades upon propagation in the link and with higher preamplifier gains. It is instructive to compare this result with the OSNR achievable in the case where the transmitter delivers sufficient power per channel, $OSNR_{laser}$, by setting $G_{pre} = 1$ in Eq. (3),

$$\frac{OSNR_{rec}}{OSNR_{laser}} = \frac{1}{1 + \frac{G_{pre} - 1}{N(G_{link} - 1)}} = \frac{1}{1 + \frac{OSNR_{laser}}{OSNR_{Tx}}} . \qquad (4)$$

The first equality indicates that the OSNR of the comb-based transmitter will be lower than the OSNR of a multi-wavelength laser-based transmitter, particularly when the gain of the preamplifier becomes comparable to or larger than the gain of the total link, $G_{pre} \sim NG_{link}$. Thus, frequency comb sources may be more suitable to operate in long-haul communication systems, where the spontaneous emission noise of the EDFAs in the link masks the limited SNR at the transmitter. In the second equality, $OSNR_{Tx} = P_{launch}/[n_{sp}h\nu\Delta\nu(G_{pre} - 1)]$ is the OSNR at the transmitter side, i.e. Eq. (3) with *N*=0. This equation assesses the penalty incurred at the receiver side due to having a limited OSNR at the transmitter. It provides a useful guideline to calculate the necessary OSNR at the transmitter side given the modulation format requirements set by in Fig. 2. This equation indicates that the OSNR at the transmitter side should be at least 13dB higher than the target OSNR at the
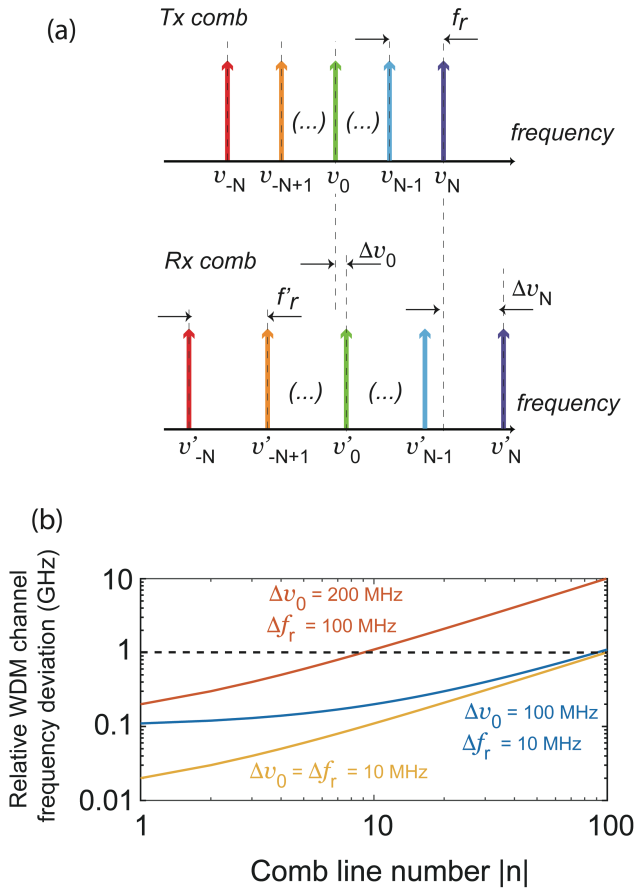
Fig. 4. (a) Schematic representation of the mismatch between Tx and Rx combs, each containing 2N+1 lines. (b) Frequency deviation as a function of the comb line number counted from the central carrier frequency. This is calculated for different offset frequencies and mismatch in repetition rates. The maximum tolerable frequency difference depends on the exact DSP algorithm, but a practical rule of thumb is to avoid deviations in the
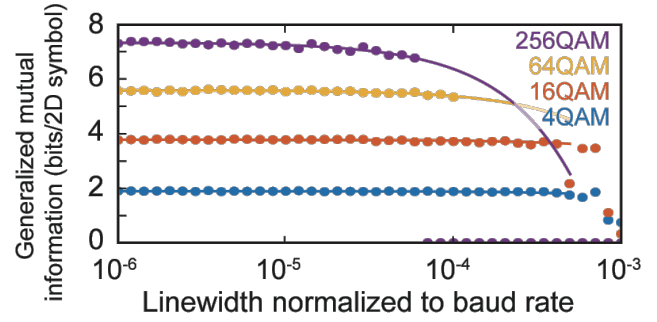

Fig. 5. Generalized mutual information (GMI) for different modulation formats as the linewidth, normalized to the baud rates, increases. For each modulation format, the SNR is kept constant, and its value close to the value that provides a BER close to 0.01, see Fig. 2. The linewidth reflects the combined effect of phase noise in the transmitter and receiver. Phase recovery is performed by the blind phase search algorithm and the drift is modeled by a Wiener process [38].

The frequency mismatch between combs is

$$\nu_n - \nu'_n = (\nu_0 - \nu'_0) + n(f_r - f'_r) = \Delta\nu_0 + n\Delta f_r. \qquad (5)$$

Here, we have assumed that the frequency difference between combs is constrained within half the repetition rate, so that the same line number can be assigned to both combs. The above equation indicates that outer lines experience higher frequency mismatch. Figure 4(b) illustrates the requirements for pairs of combs. The maximum tolerable deviation depends on the particular DSP algorithm, but a good rule of thumb is to keep the deviation to ~1 GHz or less for 10-20 Gbaud signals. Higher deviations introduce challenges in the frequency offset estimation DSP block and may lead to large performance variation and loss of data. Considering a WDM system with 20 channels, this introduces a requirement to be able to match the offset frequency and repetition rate between combs with ~ 500 MHz and 50 MHz accuracy, respectively. This may not be a problem for combs that are continuously tunable and whose repetition rate can be set by a microwave signal, such as electro-optic combs [34], but it introduces fabrication challenges for integrated frequency comb generators that rely on cavities, such as passively mode-locked lasers and microresonator combs. Notwithstanding, recent advances in dissipative Kerr solitons in silicon nitride microresonators demonstrate that it is possible to achieve these requirements with 100 GHz combs specifically designed for ultra-high channel count [35].

Optical signal processing schemes can relax these requirements and operate the receiver in a self-homodyne configuration (the local oscillator frequency matches the channel frequency), but at the expense of hardware complexity [17,36,37]. Examples include nonlinear regeneration of an electro-optic comb [36] or frequency synchronization via digital signal processing and optical feedback on a gain switched diode [37]. These examples match both the offset frequency and repetition rate and therefore synchronize the receiver comb to the transmitter. For combs whose repetition rate is sufficiently stable, locking the central line of the receiver comb is enough [17].

receiver side to suffer a penalty in the order of 0.2 dB or lower [see Fig. 3(b)].

B. Tolerable frequency mismatch between Tx and Rx combs

Figure 1 assumes a comb at the transmitter (Tx) and another one at the receiver (Rx). In the most general case, these two combs will not be locked to each other but designed with the same nominal frequencies. In this sub-section we discuss the maximum tolerable frequency difference to ensure proper operation of the digital signal processing (DSP) blocks at the Rx side in an intradyne coherent receiver (i.e. the local oscillator frequency is close but not equal to the center frequency of the WDM channel).

We consider a situation like the one sketched in Fig. 4(a), where the Tx and Rx combs are slightly mismatched in both line spacing and offset frequency. For simplicity, we label the comb frequencies as $\nu_n = \nu_0 + nf_r$, where ν_0 is the central comb line frequency, f_r the repetition rate and n an integer number denoting the sideband counted from the center. This labeling is particularly useful when considering combs that are generated from a continuous-wave laser that defines the center of the comb, such as electro-optic combs or microresonator frequency combs.
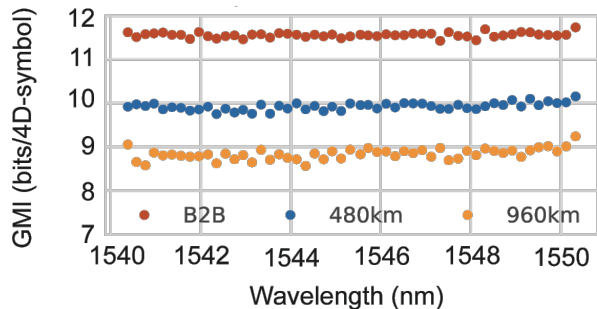
Fig. 6. Experimental example of a comb-based Tx system featuring > 10 Tb/s and 9.6 b/s/Hz spectral efficiency after 960 km propagation in a recirculating fiber loop [41]. The generalized mutual information is displayed per WDM channel and for different propagation lengths. Note that the GMI is close to the theoretical value of 12 bits/4D symbol based on Fig. 2(b) considering polarization multiplexed 64 QAM. The comb source is an electro-optic comb generator formed by cascading one intensity modulator and two phase modulators [34]. The continuous-wave laser has a nominal 100 kHz linewidth and a similar laser is used at the receiver side as tunable local oscillator. The microwave signal driving the modulators comes from a commercial low-noise dielectric resonator oscillator.

C. Absolute frequency accuracy and grid spacing

The previous sub-section concerned about matching the Rx comb lines to the Tx. A different aspect is the accuracy with which the frequency lines in the Tx must match a frequency grid. The International Telecommunication Union (ITU) regulations on dense WDM (ITU-T G.694.1) establish that the allowed channel frequencies must be anchored to 193.1 THz on a fixed grid with 12.5×2^l GHz spacing, with l being either 0, 1, 2 or 3. The nominal frequencies of the grid are defined with an accuracy that depends on the grid spacing, and it ranges from 4 digits of precision for a 12.5 GHz grid to one digit for 100 GHz. This means self-referencing is not necessary in practice and the required level of accuracy can be easily attained with e.g. free-running electro-optic comb generators or microresonator combs.

D. Optical linewidth

Advanced modulation formats are affected by phase noise from the optical source. The impact of laser phase noise in coherent communications systems has been extensively analyzed in the literature (see eg. [38,39]). Here, we give a different insight by analyzing the impact of the phase noise on the GMI for different M-ary constellations (Fig. 5). Clearly, higher-order constellations are more susceptible to phase noise because the angular separation between adjacent constellation points decreases with increased modulation order. An interesting aspect revealed by Fig. 5 is that a broader linewidth causes a continuous decrease in the GMI, but there is a point upon which the GMI drops abruptly to zero. This is due to the presence of cycle phase slips that are not handled by the blind phase-search algorithm in the DSP, which could otherwise be addressed by, e.g., differential bit encoding.

Figure 5 shows that, for baud rates in the order of 10 Gbaud and for the most complex modulation formats, the DSP can
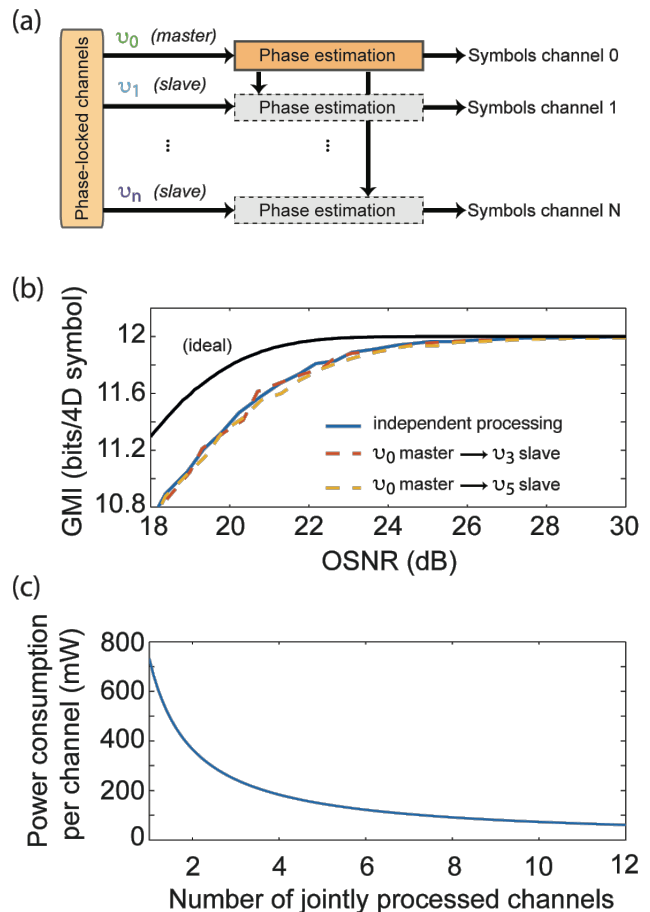

Fig. 7. (a) Principle of master-slave phase recovery. The phase is estimated from a master channel and applied to the slave channels. (b) Experimental generalized mutual information as a function of OSNR for 10 GBaud PM-64 QAM with separate and master-slave phase recovery, for two different slave channels, and compared to the case where one of the channels were processed with standard phase recovery DSP (indicated as independent). Here, the OSNR is measured in 12.5 GHz bandwidth, so a factor of 1.25 has to be considered to translate into SNR and make direct comparisons with Fig. 2. Two free-running electro-optical frequency combs with 25 GHz spacing were used as carrier and LO [43]. (c) Estimated power consumption of the phase estimation per-channel for 40 GBaud PM-64QAM as a function of the number of jointly processed channels. The power consumption values are based on an ASIC implementation of blind phase search [44].

successfully track the phase noise with minimum degradation in the GMI as long as the joint linewidth is $\sim$ 100 kHz. This linewidth is relatively easy to achieve with electro-optic comb generators because they can be pumped directly by a narrow linewidth continuous-wave laser and suffer little degradation across the bandwidth of interest in WDM communications. The situation is different for other high repetition rate frequency comb generators, such as semiconductor passively mode-locked lasers [40]. These comb sources require additional external cavities or injection locking to an external continuous-wave laser to reach optical linewidths below 1 MHz [21].

III. ADVANCES AT THE SYSTEM LEVEL

Frequency combs offer unique opportunities to increase the performance of WDM systems. To get more physical insight, it

is worth comparing the electric field of an array of individually tunable lasers with carrier frequencies ν_n and phase noise $\varphi_n(t)$,

$$E_{lasers}(t) = E \sum_{n=-N}^{N} \exp\left[-j2\pi\nu_n t + j\varphi_n(t)\right], \qquad (6)$$

with the electric field of a frequency comb

$$E_{comb}(t) = e^{-j2\pi\nu_0 t + j\varphi_0(t)} \sum_{n=-N}^{N} E_n \exp\left[-j2\pi n f_r t\right] . \quad (7)$$

Note that Eq. (6) does not represent a Fourier series since the carrier frequencies cannot be precisely located on an equidistant grid. Another important difference is that the optical phase noise in the frequency comb, as described by Eq. (7), is the same for all carrier frequencies. Hence, there are two distinct and unique aspects of a frequency comb that can be exploited for coherent communications. One is the stability of the line spacing, and the other is broadband phase coherence across a wide bandwidth.

Figure 6 shows experimental results for a comb-based superchannel Tx [41]. 51 channels are modulated by polarization multiplexed 64 QAM signals at 24 Gbaud, resulting in an achievable information rate of 11.9 Tb/s and spectral efficiency 9.3 bits/s/Hz after substracting the overhead. The signal is successfully propagated over 960 km in a recirculating loop [41]. These results are enabled by the robust line spacing in the comb source and an optimized DSP implementation using pilot symbols, which is available via an open source license [42].

Figure 7 illustrates a different example. According to Eq. (7), the optical phase noise in a comb-based system is correlated among WDM channels. This opens the door to reuse the phase noise information extracted from one WDM to the next one, see Fig. 7(a). This scheme, coined master-slave phase recovery, has been recently implemented using two free running electro-optic combs, one at the transmitter and another at the receiver [43]. Experimental results for the back-to-back situation (no propagation) are illustrated in Fig. 7(b). Essentially, the performance of the master-slave configuration is identical to the performance of the system when the phase recovery is realized on independent channels. As chromatic dispersion causes a time offset between the WDM channels, the master-slave configuration will suffer from a penalty that depends on the system length, the spectral distance between the master and the slave, and the linewidth of the comb sources. A thorough analysis of this penalty is outside the scope of this paper, but as a rule of thumb, the time offset between master and slave needs to be well below the coherence time of the comb sources, similar to self-homodyne superchannels [36]. For example, for a 100 km dispersive link and a 5 nm comb-based superchannel, this translates into a dispersive walk off of ~ 10ns. Requiring a coherence time 100 times longer demands optical frequency carriers with a linewidth below 1 MHz.

The master-slave configuration enables a substantial simplification of the DSP at the receiver and may lead to significant power savings. This is particularly interesting for short-reach links because the power used by the phase recovery
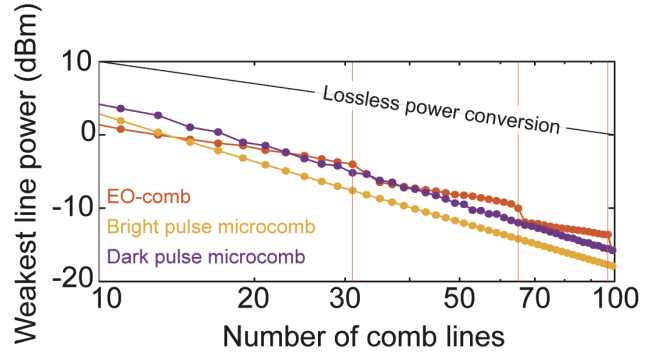

Fig. 8. Numerical simulation of the optical power achieved in the weakest (lowest) line for three different comb sources, independently optimized for a target number of comb lines. The continuous-wave pump power is 100 mW for all cases. The solid black line indicates the level corresponding to even power distribution in the case of an ideal lossless comb generator. The electro-optic (EO) comb is configured with one intensity modulator and one or more phase modulators. The solid orange vertical lines mark the point where a new phase modulator must be added to reach the target bandwidth. All combs are designed for 50 GHz line spacing. The microresonators are assumed to be implemented with stoichiometric silicon nitride with an intrinsic quality factor of ten million and following an optimization procedure as described in [54]. The EO comb is assumed to have $V_\pi \sim 4V$, 2dB loss for each modulator and a maximum RF power handling of 36 dBm (corresponding to 10 V_π). These parameters are similar to what can be obtained with state of the art commercially available lithium niobite modulators.

block in the DSP chain takes a more substantial proportion than in long-haul systems. An estimate of the power savings is provided in Fig. 7(c), indicating an exponential decrease of the power consumption of the phase recovery unit with the number of jointly processed WDM channels [44].

IV. PROGRESS IN MICRORESONATOR FREQUENCY COMBS

The results highlighted in the previous section were realized with electro-optic frequency comb generators (or EO combs in short). From a practical point of view, realizing comb-based WDM coherent transmitters and receivers will require a large degree of photonic integration. Microresonator frequency combs (or microcombs in short) developed using silicon nitride [45] offer a path forward in combination with advances in silicon photonics [46]. Here, we establish a brief comparative assessment between these two comb technologies for applications in WDM.

Both microcombs and EO combs are seeded by a continuous-wave laser. If this laser has sufficiently low linewidth, it is safe to neglect potential phase noise variations from one WDM channel to another. In fact, both platforms have demonstrated successful transmission of advanced modulation formats [17,35,47,48].

Next, we focus our attention on the power achieved in the weakest comb line, P_{low}. This figure of merit implicitly considers absorption losses in the comb generation process and uneven power distribution among lines. The results are presented in Fig. 8. The EO comb is modelled by considering an intensity modulator followed by a set of phase modulators [49]. For microcombs, we consider two different generation processes i.e., dissipative Kerr solitons [50], which have a very

smooth spectral envelope but relatively poor power conversion efficiency [51], and mode-locked dark pulses [52], which feature much higher conversion efficiency [53] but at the expense of large power variations among lines. The microresonators are optimized in terms of coupling rate and dispersion [35,54], considering intrinsic quality factors of ten million, which can be realized based on recent fabrication developments [55,56]. This analysis indicates that optimized mode-locked dark pulses can approach a performance in terms of power per line very close to what can be achieved with state of the art, commercially available electro-optic comb generators based on lithium niobate. Recent results based on lithium niobate on insulator could yield higher comb line powers assuming they could sustain high RF powers and maintain low propagation losses [57].

The above results indicate that power per lines ranging between 0 to -10 dBm are feasible for integrated combs containing ~ 15-50 lines. This translates into OSNRs per WDM channel (0.1nm bandwidth) in the order of 31-41 dB at the transmitter side, assuming a setup like the one in Fig. 1 could be implemented with ~15 dB loss per channel without optical amplifiers between the comb and multiplexers.

With regards to line spacing stability, it is worth emphasizing that dissipative Kerr solitons in whispering gallery mode resonators can provide a photodetected radio-frequency beat note whose phase noise [58] is better than the performance of the phase noise of the dielectric resonator oscillators driving the electro-optic combs used in the previous section. Further research is needed to understand whether a similar performance level could be achieved with mode-locked dark pulses generated in silicon nitride microresonators.

V. SUMMARY

A single frequency comb can replace tens of lasers in a WDM system. The combs can be used at the transmitter side as a multi-carrier source on which to encode complex data, and at the receiver side as a phase-locked multi-wavelength local oscillator. The limited power per line in a comb results in a received signal with lower OSNR, but this aspect becomes less of a concern for longer links, where the performance is dominated by the noise in the amplifiers of the link. The ITU demands in terms of absolute frequency accuracy are not particularly stringent and can be easily met with standard comb sources used in communication systems. Matching Tx and Rx frequencies requires positioning the lines with ~100 MHz relative accuracy, which introduces challenges for combs that rely on cavity waveguides. Finally, the optical phase noise requirements for the most demanding modulation formats considered in this work can be met with 100 kHz linewidths.

With regards to recent advances at the system level, we have shown the possibility to achieve spectral efficiencies close to 10b/s/Hz over transmission distances ~1000 km and achievable information rates > 10 Tb/s. These results are implemented with electro-optic combs, whose line spacing stability allows decreasing the guardbands between WDM channels. In a different example, we have shown how the broadband phase coherence of electro-optic combs can be utilized to realize a fully coherent WDM link, with significant simplifications of the DSP blocks. This can result in notable power savings, depending on the number of processed channels.

Finally, we discussed how mode-locked dark pulse combs in silicon nitride microresonators can potentially provide powers per line close to what can be achieved with state-of-the-art, but bulky and power hungry, electro-optic frequency comb generators.

REFERENCES

[1] D. J. Jones, S. A. Diddams, J. K. Ranka, A. Stentz, R. S. Windeler, J. L. Hall, and S. T. Cundiff, "Carrier-envelope phase control of femtosecond mode-locked lasers and direct optical frequency synthesis," *Science*, vol. 288, no. 5466, pp. 635–639, April 2000.

[2] R. Holzwarth, T. Udem, T. W. Hänsch, J. C. Knight, W. J. Wadsworth, and P. St. J. Russell, "Optical frequency synthesizer for precision spectroscopy," *Phys. Rev. Lett.*, vol. 85, no. 11, pp. 2264–2267, Sept. 2000.

[3] A. D. Ludlow, M. M. Boyd, J. Ye, E. Peik, and P. O. Schmidt, "Optical atomic clocks," *Rev. Mod. Phys.*, vol. 87, no. 637, June 2015.

[4] I. Coddington, W. Swann, and N. Newbury, "Coherent multiheterodyne spectroscopy using stabilized optical frequency combs," *Phys. Rev. Lett.*, vol. 100, no. 1, pp. 013902–4, Jan. 2008.

[5] T. M. Fortier, M. S. Kirchner, F. Quinlan, J. Taylor, J. C. Bergquist, T. Rosenband, N. Lemke, A. Ludlow, Y. Jiang, C. W. Oates, and S. A. Diddams, "Generation of ultrastable microwaves via optical frequency division," *Nature Photon.*, vol. 5, no. 7, pp. 425–429, July 2011.

[6] I. Coddington, W. C. Swann, L. Nenadovic, and N. R. Newbury, "Rapid and precise absolute distance measurements at long range," *Nature Photon.*, vol. 3, no. 6, pp. 351–356, May 2009.

[7] J. J. Veselka and S. K. Korotky, "A multiwavelength source having precise channel spacing for WDM systems," *IEEE Photon. Technol. Lett.*, vol. 10, no. 7, pp. 958–960, Jul. 1998.

[8] T. Ohara *et al.*, "Over-1000-channel ultradense WDM transmission with supercontinuum multicarrier source," *J. Lightwave Technol.*, vol. 24, no. 6, pp. 2311–2317, May 2006.

[9] V. Ataie et al., "Ultrahigh count coherent WDM channels transmission using optical parametric comb-based frequency synthesizer," *J. Lightwave Technol.*, vol. 33, no. 3, pp. 694–699, Feb. 2015.

[10] M. Mazur, A. Lorences-Riesgo, J. Schröder, P. A. Andrekson, and M. Karlsson, "10 Tb/s PM-64QAM self-Homodyne comb-based superchannel transmission with 4% shared pilot tone overhead," *J. Lightwave Technol.*, vol. 36, no. 16, pp. 3176–3184, Aug. 2018.

[11] B. J. Puttnam, R. S. Luís, W. Klaus, J. Sakaguchi, J. M. D. Mendinueta, Y. Awaji, N. Wada, Y. Tamura, T. Hayashi, M. Hirano, and J. Marciante, "2.15 Pb/s transmission using a 22-core homogeneous single-mode multi-core fiber and wideband optical comb," *Proc. ECOC*, Valencia, Spain, 2015, pp. 1–3.

[12] A. D. Ellis and F. C. G. Gunning, "Spectral density enhancement using coherent WDM," *IEEE Photon. Technol. Lett.*, vol. 17, no. 2, pp. 504–506, Jan. 2005.

[13] E. Yamazaki, F. Inuzuka, K. Yonenaga, A. Takada, and M. Koga, "Compensation of interchannel crosstalk induced by optical fiber nonlinearity in carrier phase-locked WDM system," *IEEE Photon. Technol. Lett.*, vol. 19, no. 1, pp. 9–11, Feb. 2007.

[14] E. Temprana, E. Myslivets, B. P. P. Kuo, L. Liu, V. Ataie, N. Alic, and S. Radic, "Overcoming Kerr-induced capacity limit in optical fiber transmission," *Science*, vol. 348, no. 6242, pp. 1445–1448, June 2015.

[15] E. Temprana, E. Myslivets, L. Liu, V. Ataie, A. Wiberg, B. P. P. Kuo, N. Alic, and S. Radic, "Two-fold transmission reach enhancement enabled by transmitter-side digital backpropagation and optical frequency comb-derived information carriers," *Opt. Express*, vol. 23, no. 16, pp. 20774–20783, Aug. 2015.

[16] D. Hillerkuss, R. Schmogrow, M. Meyer, S. Wolf, M. Jordan, P. Kleinow, N. Lindenmann, P. C. Schindler, A. Melikyan, X. Yang, S. Ben-Ezra, B. Nebendahl, M. Dreschmann, J. Meyer, F. Parmigiani, P. Petropoulos, B. Resan, A. Oehler, K. Weingarten, L. Altenhain, T. Ellermeyer, M. Moeller, M. Huebner, J. Becker, C. Koos, W. Freude, and J. Leuthold, "Single-Laser 325 Tbit/s Nyquist WDM Transmission," *J. Opt. Commun. Netw.*, vol. 4, no. 10, pp. 715–9, Oct. 2012.

[17] M. Mazur, A. Lorences-Riesgo, J. Schröder, P. A. Andrekson, and M. Karlsson, "High spectral efficiency PM-128QAM comb-based superchannel transmission enabled by a single shared optical pilot tone," *J. Lightwave Technol.*, vol. 36, no. 6, pp. 1318–1325, March 2018.

[18] M. Imran, P. M. Anandarajah, A. Kaszubowska-Anandarajah, N. Sambo and L. Potí, "A survey of optical carrier generation techniques for terabit capacity elastic optical networks," in *IEEE Communications Surveys & Tutorials*, vol. 20, no. 1, pp. 211-263, First quarter 2018.

[19] V. Torres-Company and A. M. Weiner, "Optical frequency comb technology for ultra-broadband radio-frequency photonics," *Laser & Photon. Rev.*, vol. 8, no. 3, pp. 368–393, May 2014.

[20] J. Pfeifle, V. Vujicic, R. T. Watts, P. C. Schindler, C. Weimann, R. Zhou, W. Freude, L. P. Barry, and C. Koos, "Flexible terabit/s Nyquist-WDM super-channels using a gain-switched comb source," *Opt. Express*, vol. 23, no. 2, pp. 724–15, 2015.

[21] J. N. Kemal, P. Marin-Palomo, K. Merghem, A. Guy, C. Calo, R. Brenot, F. Lelarge, A. Ramdane, S. Randel, W. Freude, and C. Koos, "32QAM WDM transmission using a quantum-dash passively mode-locked laser with resonant feedback," presented at the *OFC* Postdeadline Papers, Washington, D.C., p. Th5C.3, 2017.

[22] H. Hu, F. Da Ros, M. Pu, F. Ye, K. Ingerslev, E. Porto da Silva, M. Nooruzzaman, Y. Amma, Y. Sasaki, T. Mizuno, Y. Miyamoto, L. Ottaviano, E. Semenova, P. Guan, D. Zibar, M. Galili, K. Yvind, T. Morioka, and L. K. Oxenlowe, "Single-source chip-based frequency comb enabling extreme parallel data transmission," *Nature Photon.*, vol. 12, no. 8, pp. 469–473, Aug. 2018.

[23] J. Pfeifle, V. Brasch, M. Lauermann, Y. Yu, D. Wegner, T. Herr, K. Hartinger, P. Schindler, J. Li, D. Hillerkuss, R. Schmogrow, C. Weimann, R. Holzwarth, W. Freude, J. Leuthold, T. J. Kippenberg, and C. Koos, "Coherent terabit communications with microresonator Kerr frequency combs," *Nature Photon.*, vol. 8, no. 5, pp. 375–380, May 2014.

[24] A. Fülöp, M. Mazur, A. Lorences-Riesgo, T. A. Eriksson, P.-H. Wang, Y. Xuan, D. E. Leaird, M. Qi, P. A. Andrekson, A. M. Weiner, and V. Torres-Company, "Long-haul coherent communications using microresonator-based frequency combs," *Opt. Express*, vol. 25, no. 22, pp. 26678–11, Oct. 2017.

[25] L. Lundberg, M. Karlsson, A. Lorences-Riesgo, M. Mazur, V. Torres-Company, J. Schröder, and P. Andrekson, "Frequency comb-based WDM transmission systems enabling joint signal processing," *Applied Sciences*, vol. 8, no. 5, pp. 718–25, May 2018.

[26] V. Torres-Company and A. Fülöp, "Laser frequency combs for coherent optical communications," presented at the *ECOC*, Rome, Italy, paper We3H.5, 2018.

[27] F. Kish *et al.*, "System-on-chip photonic integrated circuits," *IEEE J. Select. Topics Quantum Electron.*, vol. 24, no. 1, pp. 1–20, Jan. 2018.

[28] K. Kikuchi, "Fundamentals of coherent optical fiber communications," *J. Lightwave Technol.*, vol. 34, no. 1, pp. 157–179, Jan. 2016.

[29] P. J. Winzer, "High-spectral-efficiency optical modulation formats," *J. Lightwave Technol.*, vol. 30, no. 24, pp. 3824–3835, Dec. 2012.

[30] M. Karlsson and E. Agrell, "Multidimensional modulation and coding in optical transport," *J. Lightwave Technol.*, vol. 35, no. 4, pp. 876–884, Feb. 2017.

[31] A. Alvarado, E. Agrell, D. Lavery, R. Maher and P. Bayvel, "Replacing the soft-decision FEC limit paradigm in the design of optical communication systems," *J. Lightwave Technol.*, vol. 33, no. 20, pp. 4338-4352, Oct. 2015.

[32] R. A. Shafik, Md. S. Rahman, and A. R. Islam, "On the extended relationships among EVM, BER and SNR as performance metrics," presented at the 4th International Conf. Electrical and Computer Eng., pp. 408-411, Dec. 2006. DOI: 10.1109/ICECE.2006.355657

[33] G. P. Agrawal, "Loss management," in *Fiber-Optic Communication Systems*, Fourth Edi., Hoboken, NJ, USA: John Wiley & Sons, Inc., 2011, ch. 7, pp. 295–344. DOI: 10.1002/ 9780470918524.ch7.

[34] A. J. Metcalf, V. Torres-Company, D. E. Leaird, and A. M. Weiner, "High-power broadly tunable electrooptic frequency comb generator," *IEEE J. Select. Topics Quantum Electron.*, vol. 19, no. 6, p. 3500306, Nov. 2013.

[35] P. Marin-Palomo, J. N. Kemal, M. Karpov, A. Kordts, J. Pfeifle, M. H. P. Pfeiffer, P. Trocha, S. Wolf, V. Brasch, M. H. Anderson, R. Rosenberger, K. Vijayan, W. Freude, T. J. Kippenberg, and C. Koos, "Microresonator-based solitons for massively parallel coherent optical communications," *Nature*, vol. 546, no. 7657, pp. 274–279, June 2017.

[36] A. Lorences-Riesgo, T. A. Eriksson, A. Fülöp, P. A. Andrekson, and M. Karlsson, "Frequency-comb regeneration for self-homodyne

[37] J. N. Kemal, J. Pfeifle, P. Marin-Palomo, M. D. G. Pascual, S. Wolf, F. Smyth, W. Freude, and C. Koos, "Multi-wavelength coherent transmission using an optical frequency comb as a local oscillator," *Opt. Express*, vol. 24, no. 22, pp. 25432–14, Oct. 2016.

[38] T. Pfau, S. Hoffmann, and R. Noe, "Hardware-efficient coherent digital receiver concept with feedforward carrier recovery for m-QAM constellations," *J. Lightwave Technol.*, vol. 27, no. 8, pp. 989–999, Apr. 2009.

[39] A. Kakkar, J. R. Navarro, R. Schatz, X. Pang, O. Ozolins, A. Udalcovs, H. Louchet, S. Popov, and G. Jacobsen, "Laser frequency noise in coherent optical systems: spectral regimes and impairments," *Sci. Rep.*, 7:844, pp. 1–10, Apr. 2017.

[40] P. Marin, J. Pfeifle, J. N. Kemal, S. Wolf, K. Vijayan, N. Chimot, A. Martinez, A. Ramdane, F. Lelarge, C. Koos, and W. Freude, "8.32 Tbit/s coherent transmission using a quantum-dash mode-locked laser diode," presented at the *CLEO*, Th3F.6, 2016.

[41] M. Mazur, J. Schröder, A. Lorences-Riesgo, M. Karlsson, and P. A. Andrekson, "Optimization of low-complexity pilot-based DSP for high spectral efficiency 51x24 Gbaud PM-64 QAM transmission", presented at *ECOC*, Rome, Italy, paper MoF4.2, 2018.

[42] J. Schröder and M. Mazur, "QAMPy a DSP chain for optical communications", DOI: 10.5281/zenodo.1195720".

[43] L. Lundberg et al., "Joint carrier recovery for DSP complexity reduction in frequency comb-based superchannel transceivers," Proc. *ECOC*, Gothenburg, Sweden, Th.1.D.3, 2017.

[44] L. Lundberg, E. Börjeson, C. Fougstedt, M. Mazur, M. Karlsson, P. A. Andrekson and P. Larsson-Edefors "Power consumption savings through joint carrier recovery for spectral and spatial superchannels", presented at *ECOC*, Rome, Italy, We2.26, 2018.

[45] J. S. Levy, A. Gondarenko, M. A. Foster, A. C. Turner-Foster, A. L. Gaeta, and M. Lipson, "CMOS-compatible multiple-wavelength oscillator for on-chip optical interconnects," *Nature Photon.*, vol. 4, no.1, pp. 37–40, Jan, 2010.

[46] W. D. Sacher, Z. Yong, J. C. Mikkelsen, A. Bois, Y. Yang, J. C. Mak, P. Dumais, D. Goodwill, C. Ma, J. Jeong, E. Bernier, and J. K. Poon, "Multilayer silicon nitride-on-silicon integrated photonic platform for 3D photonic circuits," presented at *CLEO*, San Jose, CA, USA, paper JTh4C.3, Jun. 2016.

[47] A. Fülöp, M. Mazur, A. Lorences-Riesgo, Ó. B. Helgason, P.-H. Wang, Y. Xuan, D. E. Leaird, M. Qi, P. A. Andrekson, A. M. Weiner, and V. Torres-Company, "High-order coherent communications using mode-locked dark-pulse Kerr combs from microresonators," *Nature Commun.*, vol. 9, no. 1, p. 1598, Apr. 2018.

[48] P. Liao, C. Bao, A. Kordts, M. Karpov, M. H. P. Pfeiffer, L. Zhang, C. A. O. Yinwen, A. Almaiman, A. Mohajerin-Ariaei, F. Alishahi, A. Fallahpour, K. Zou, M. Tur, T. J. Kippenberg, and A. E. Willner, "Effects of erbium-doped fiber amplifier induced pump noise on soliton Kerr frequency combs for 64-quadrature amplitude modulation transmission," *Opt. Lett.*, vol. 43, no. 11, pp. 2495–2498, Jun. 2018.

[49] V. Torres-Company, J. Lancis, and P. Andres, "Lossless equalization of frequency combs," *Opt. Lett.*, vol. 33, no. 16, pp. 1822-1824, Aug. 2008.

[50] T. Herr, V. Brasch, J. D. Jost, C. Y. Wang, N. M. Kondratiev, M. L. Gorodetsky, and T. J. Kippenberg, "Temporal solitons in optical microresonators," *Nature Photon.*, vol. 8, no. 2, pp. 145–152, Dec. 2013.

[51] C. Bao, L. Zhang, A. Matsko, Y. Yan, Z. Zhao, G. Xie, A. M. Agarwal, L. C. Kimerling, J. Michel, L. Maleki, and A. E. Willner, "Nonlinear conversion efficiency in Kerr frequency comb generation," *Opt. Lett.*, vol. 39, no. 21, pp. 6126–4, Nov. 2014.

[52] X. Xue, Y. Xuan, Y. Liu, P.-H. Wang, S. Chen, J. Wang, D. E. Leaird, M. Qi, and A. M. Weiner, "Mode-locked dark pulse Kerr combs in normal-dispersion microresonators," *Nature Photon.*, vol. 9, no. 9, pp. 594–600, 2015.

[53] X. Xue, P.-H. Wang, Y. Xuan, M. Qi, and A. M. Weiner, "Microresonator Kerr frequency combs with high conversion efficiency," *Laser & Photon. Rev.*, vol. 11, no. 1, p. 1600276, 2017.

[54] Ó. B. Helgason, A. Fülöp, J. Schröder, P. A. Andrekson, A. M. Weiner, and V. Torres-Company, "Superchannel engineering with microresonator Combs," in *CLEO*, San Jose, CA, USA, paper JW2A.71, 2018.

[55] Y. Xuan, Y. Liu, L. T. Varghese, A. J. Metcalf, X. Xue, P.-H. Wang, K. Han, J. A. Jaramillo-Villegas, A. Al Noman, C. Wang, S. Kim, M. Teng, Y. J. Lee, B. Niu, L. Fan, J. Wang, D. E. Leaird, A. M. Weiner, and M. Qi, "High-Q silicon nitride microresonators exhibiting low-power

frequency comb initiation," *Optica*, vol. 3, no. 11, pp. 1171–10, Nov. 2016.

[56] M. H. P. Pfeiffer, J. Liu, A. S. Raja, T. Morais, B. Ghadiani, and T. J. Kippenberg, "Ultra-smooth silicon nitride waveguides based on the Damascene reflow process: fabrication and loss origins," *Optica*, vol. 5, no. 7, pp. 884–892, Jul. 2018.

[57] M. Zhang, C. Wang, B. Buscaino, A. Shams-Ansari, J. M. Kahn, and M. Loncar, "Electro-optic frequency comb generation in ultrahigh-Q integrated lithium niobate microresonators", presented at *CLEO*, San Jose, CA, paper FW3E.4, 2018.

[58] W. Liang, D. Eliyahu, V. S. Ilchenko, A. A. Savchenkov, D. Seidel, L. Maleki, and A. B. Matsko, "High spectral purity Kerr frequency comb radio frequency photonic oscillator," *Nature Commun.*, vol. 6, p. 7957, Aug. 2015.